Molecular Biology of the Cell
Vol. 8, 1763–1775, September 1997

Chemotaxis to cAMP and Slug Migration in *Dictyostelium* Both Depend on MigA, a BTB Protein

Ricardo Escalante,* Deborah Wessels,† David R. Soll,† and William F. Loomis*‡

*Center for Molecular Genetics, Department of Biology, University of California San Diego, La Jolla, California 92093; and †Department of Biological Sciences, University of Iowa, Iowa City, Iowa 52242

Submitted February 21, 1997; Accepted June 3, 1997
Monitoring Editor: Peter Devreotes

Chemotaxis in natural aggregation territories and in a chamber with an imposed gradient of cyclic AMP (cAMP) was found to be defective in a mutant strain of *Dictyostelium discoideum* that forms slugs unable to migrate. This strain was selected from a population of cells mutagenized by random insertion of plasmids facilitated by introduction of restriction enzyme (a method termed restriction enzyme-mediated integration). We picked this strain because it formed small misshapen fruiting bodies. After isolation of portions of the gene as regions flanking the inserted plasmid, we were able to regenerate the original genetic defect in a fresh host and show that it is responsible for the developmental defects. Transformation of this recapitulated mutant strain with a construct carrying the full-length *migA* gene and its upstream regulatory region rescued the defects. The sequence of the full-length gene revealed that it encodes a novel protein with a BTB domain near the N terminus that may be involved in protein–protein interactions. The *migA* gene is expressed at low levels in all cells during aggregation and then appears to be restricted to prestalk cells as a consequence of rapid turnover in prespore cells. Although *migA*$^-$ cells have a dramatically reduced chemotactic index to cAMP and an abnormal pattern of aggregation in natural waves of cAMP, they are completely normal in size, shape, and ability to translocate in the absence of any chemotactic signal. They respond behaviorally to the rapid addition of high levels of cAMP in a manner indicative of intact circuitry connecting receptor occupancy to restructuring of the cytoskeleton. Actin polymerization in response to cAMP is also normal in the mutant cells. The defects at both the aggregation and slug stage are cell autonomous. The MigA protein therefore is necessary for efficiently assessing chemical gradients, and its absence results in defective chemotaxis and slug migration.

INTRODUCTION

Cell movement is an important step in the development of many multicellular organisms. *Dictyostelium* cells have to move together to form aggregates and then move relative to each other within the aggregates to sort out prestalk cells to the anterior so that they can direct the subsequent movement of slugs (Loomis, 1975, 1982, 1996; Traynor *et al.*, 1992). The direction of movement during aggregation is controlled by chemotactic responses to cyclic AMP (cAMP; Chen *et al.*, 1996; Parent and Devreotes, 1996). cAMP is bound on the surface of the cells by a seven transmembrane receptor connected to several signal transduction pathways. A G-protein-dependent pathway couples receptor occupancy via the protein adaptator cystolic regulator of adenylyl cyclase (CRAC) to activation of adenylyl cyclase (Insall *et al.*, 1994). cAMP is released in a pulsatile manner from an aggregation center, and the signal is relayed outwardly through the cell population as a nondissipating relatively symmetrical wave. Relay includes the adaptation of cAMP receptors. A cAMP phosphodiesterase rapidly degrades extracellular cAMP, allowing reactivation of the recep-

‡ Corresponding author.

tor. Receptor occupancy also results in activation of guanylyl cyclase, resulting in a transient rise in cGMP that has been implicated in restructuring of the cytoskeleton and wave propagation (Kuwayama *et al.*, 1993; Chandrasekhar *et al.*, 1995).

Many of the genes involved in cAMP responses during aggregation are induced by extracellular pulses of cAMP. Later, when cells have entered mounds, the concentration of cAMP rises above a threshold necessary for expression of postaggregation genes (Firtel, 1995). Expression of these genes is also dependent on accumulation of a specific transcription factor, G-box binding factor (GBF) (Schnitzler *et al.*, 1994). The cAMP-dependent protein kinase, protein kinase A, plays multiple roles during aggregation as well as at later stages (Harwood *et al.*, 1992; Bonner and Williams, 1994; Reymond *et al.*, 1995). Thus, the levels of cAMP within cells control many aspects of progression through the developmental stages.

Prespore and prestalk cells differentiate at random positions within aggregates and then sort out such that the prestalk cells are found at the top of the mounds where they form a tip (Williams *et al.*, 1989; Williams and Jermyn, 1991). It has been suggested that prestalk cells are attracted to cAMP, which is thought to be higher at the tip (Traynor *et al.*, 1992). However, prestalk cells sort to the surface before moving to the top and it is not clear that gradients of cAMP could account for this trajectory. Other possibilities include differential adhesion between cells and interactions with the extracellular matrix.

It has also been suggested that slug migration is mediated by chemotaxis to cAMP (Siegert and Weijer, 1992, 1995; Bretschneider *et al.*, 1995). Slugs are phototactic and move toward light under the control of prestalk cells at the anterior where the sheath can be distended (Francis, 1964). When a slug migrates, prespore cells in the posterior move in concert with the overall structure but prestalk cells rotate around the long axis and so follow a spiral trajectory. Although some evidence for pulses can be seen in the movement of prestalk cells as they spiral around, it is not clear that they represent responses to cAMP. Moreover, spirals cannot be seen in the movement of prestalk cells of certain strains suggesting that they may not be necessary for slug migration (Siegert and Weijer, 1995).

We have isolated a mutant strain of *Dictyostelium* in which the cells have a dramatically reduced ability to respond to gradients of cAMP but can move randomly in a manner indistinguishable from that seen in wild-type cells in the absence of a gradient of cAMP. Slugs formed from cells of this mutant strain are completely unable to migrate, suggesting that the disrupted gene plays roles in both chemotactic aggregation and slug migration. Because the mutant strain was generated by restriction enzyme-mediated integration, the integrated plasmid could be rapidly isolated with its flanking regions from the disrupted gene *migA*. The sequence of the gene indicates that it encodes a novel protein with a BTB domain at the N terminus. Further characterization of the phenotype of null mutants indicated that sorting out of prestalk cells occurred normally in mounds of the mutant cells and that the defects in both aggregation and slug migration are cell autonomous.

MATERIALS AND METHODS

Cells, Growth, Transformation, and Development

Innocula of wild-type and *migA*$^-$ cells were thawed from frozen stocks every 3 wk and grown axenically in HL5 medium (Sussman, 1987). Transformations were carried out as described by Kuspa and Loomis (1992) and G418- and blasticidin-resistant transformants were selected as previously described (Shaulsky and Loomis, 1993; Adachi *et al.*, 1994). Strains were cloned from plaques that grew on SM plates spread with *Klebsiella aerogenes* (Sussman, 1987). Development on filters, slug migration on agar plates, and detergent treatment of spores were performed as described by Shaulsky and Loomis (1993), except in the case of motion analysis experiments, where development was performed as described by Soll (1987).

Motion Analysis

Cells at the ripple stage were gently washed off filters after 6.5–7 h of development and suspended in BSS (20 mM KCl, 2.4 mM $MgCl_2$, 20 mM KH_2PO_4, 20 mM Na_2HPO_4, pH 6.4) at 3×10^4 cells/ml. Cells were deposited in a Sykes-Moore perfusion chamber and allowed to adher for 5 min before being perfused with BSS at 4 ml/min at 22°C (Varnum *et al.*, 1986). Movements of individual cells were recorded on half-inch videotape for a minimum of 10 min at a magnification of 250× by using bright-field optics. Morphology and motility parameters were digitized and computed by 2D-DIAS as previously described (Soll, 1995; Soll and Voss, 1997).

Chemotaxis was assessed in a spatial gradient of cAMP established across a 2-mm bridge separating a source and a sink (Zigmond, 1977; Varnum and Soll, 1984). BSS containing 10^{-6} M cAMP was placed in the source trough and BSS alone was placed in the sink trough. Cells were dispersed on the bridge and allowed to acclimate for 8 min before being video recorded. The chemotactic index was computed from the centroid track of the cell as the net distance moved directly toward the source divided by the total distance moved (Varnum and Soll, 1984). A value of +1.0 indicates perfect tracking toward the source, and a value of −1.0 indicates persistent movement away from the source.

Vector Analysis of Behavior in Natural cAMP Waves

Exponentially growing cells were washed free of nutrients and suspended in BSS at 2.4×10^6 cells/ml. Two milliliters of the suspension were added to a 35-mm tissue culture dish coated with 300 μl of 1% Noble agar in BSS. After 30 min, 1 ml was carefully withdrawn and the dish was placed on the stage of a Zeiss ICM405 inverted microscope where a field was selected by using the 10× objective and bright-field optics. Low-light images were recorded onto half-inch videotape for up to 10 h through a Cooled-Coupled Charge Device camera (Optronics, Goleta, CA). Images were analyzed by using a newly developed 3D-DIAS vector flow program (Soll, 1995; Soll and Voss, 1997). In this program, a kernel of 5×5 pixels is centered over an arbitrary point in the current video frame F. That kernel rectangle is then superimposed over all points within a threshold distance of 5 pixels from the original point in the next

video frame F + 1. The best match using pixel intensity of all such rectangles in frame F + 1 with the original kernel rectangle in frame F is found. The criterion for the match is based on the mean and SD of differences of corresponding pixel intensities. An arrow is then constructed connecting the original point in frame F with the center of the best matching rectangle in frame F + 1. This arrow is called the vector flow arrow. Its length measures the distance that a localized region of pixel detail has moved in one frame. For vector analysis, arrows are constructed at every point in a video frame and averaged by using a Tukey window to remove noise. To obtain a single numerical value representing average flow at a given frame, the user selects a rectangular region of interest in which the magnitudes of the flow vectors are averaged. The user selects a direction of interest, for example, the direction toward the aggregation center. The magnitudes of the vector component of the flow arrows parallel to that given direction are averaged and plotted over time. The Y-axis of these plots measures the mean velocity component in the direction of aggregation of a field of cells.

Nucleic Acid Manipulation

Genomic DNA was prepared and analyzed on Southern blots as described by Kuspa and Loomis (1992). RNA was prepared at different developmental stages by using the Trizol reagent (Life Technologies, Gaithersburg, MD). Poly(A)$^+$ RNA was bound and eluted from poly(dT) cellulose before being electrophoretically separated on 1% agarose gels containing 2.2 M formaldehyde. RNA was transferred to nylon membrane (Magna Graph Nylon, MSI, San Diego, CA) for hybridization. Standard methods of cloning and nucleic acid manipulation were carried out according to Ausubel (1992) and Sambrook *et al.* (1989).

Molecular Cloning of migA, Sequence Analysis, and DNA Constructs

cDNA clones were recognized in a cDNA library prepared from RNA of cells developed to the slug stage (Shaulsky *et al.*, 1995) by probing with a *migA* genomic fragment that encodes aa 628 to aa 787. Both strands of genomic and cDNA clones were sequenced on an Applied Biosystems Prism 377 DNA sequencer (Foster City, CA). Database searches were determined with the BLAST program (Altschul *et al.*, 1990).

The *migA* gene was disrupted by homologous recombination with a plasmid obtained by cutting the genomic DNA of DG1020 with the restriction enzyme *Nde*I. The *migA* gene was deleted by homologous recombination with this plasmid after cutting with *Xba*I and *Swa*I and religating. This step removed the coding sequences upstream of the insertion site in DG1020.

A rescue vector was prepared by cloning a 3.6-kb portion of *migA* into *Sal*I/*Xba*I-digested pDXA plasmid (Manstein *et al.*, 1995). The *migA* sequence contains 1.8 kb of the 5′ untranslated region, the complete coding region with its intron, and the 3′ untranslated region cloned from cDNA. Two reporter constructs in which β-galactosidase is under the control of the *migA* regulatory region were constructed by ligating portions of *migA* to plasmid pDdGal16 (Harwood and Drury, 1990). In the first construct the *Eco*RI–*Bgl*II fragment of *migA* that contains the 5′ untranslated sequence and the first 130 codons was used, and a second construct a polymerase chain reaction-generated fragment that contains the 5′ untranslated sequence and only the first two codons was used.

Filamentous Actin (F-Actin) Measurement

Nitrobenzene-phallicidin binding to F-actin was measured in cells before and after addition of cAMP as described by Hall *et al.* (1988).

cAMP Induction

Axenically grown cells were washed and suspended at 5×10^6 cells/ml in 20 mM phosphate buffer, pH 6.2, and shaken at 200 rpm.

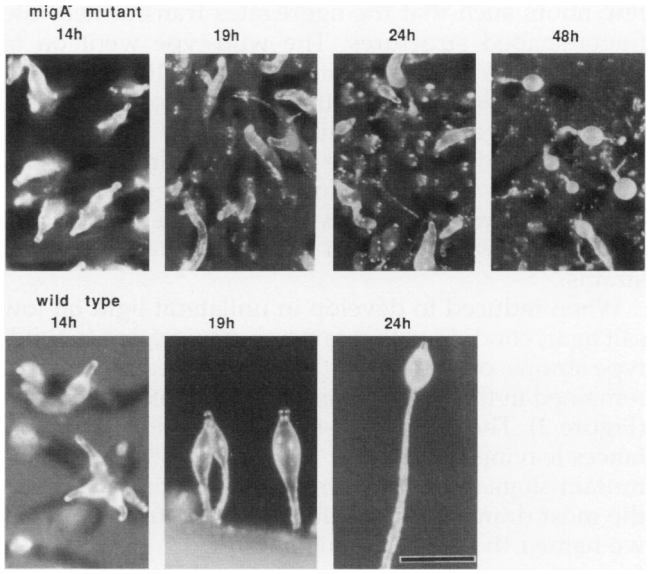

Figure 1. Developmental morphology. Cells of strains DG1020 (*migA*$^-$) and AX4 (*migA*$^+$) were grown axenically, washed, and deposited on buffer-saturated filters for development. Structures were photographed after the indicated times (hours). Bar, 0.4 mm.

After 6 h, 300 μM cAMP were added to half the cells and the flasks were shaken at 130 rpm for an additional 6 h. Cells treated with cAMP received additional cAMP to 150 μM every 2 h. The cells were collected for RNA isolation after 10 and 12 h in suspension.

In Situ Hybridization and 5-Bromo-4-chloro-3-indolyl β-D-Galactoside (X-gal) Staining

Riboprobes from Dd63 (*ecmA*; Jermyn *et al.*, 1989), Dd56 (*ecmB*; Williams *et al.*, 1989), and cotB-70.5 (*cotB*; Fosnaugh and Loomis, 1989) were labeled with digoxygenin by using the DIG RNA labeling kit from Boehringer Mannheim (Indianapolis, IN). Probes were partially hydrolyzed and hybridized to fixed samples, and bound probe were detected as described by Escalante and Loomis (1995). The *cotB* probe was hybridized at 50°C and the *ecmA* and *ecmB* probes were hybridized at 60°C to avoid cross-hybridization. Samples were washed for 30-min periods sequentially in 2× SSC, 1× SSC, 0.2× SSC, and 0.1 SSC at the hybridization temperature.

RESULTS

Isolation and Gross Phenotype of Strain DG1020

Strain DG1020 was isolated from a screen of morphological mutants of *Dictyostelium discoideum* strain AX4 generated by the insertion of the pBSr plasmid by using restriction enzyme-mediated integration (Kuspa and Loomis, 1992; Adachi *et al.*, 1994). When developed at a high cell density on buffer-saturated filters, cells of this strain formed small aggregates that proceeded slowly through morphogenesis (Figure 1). Although they aggregated at the expected time (10 h), the loose aggregates failed to coalesce as they formed tight aggregates and so remained at about half the size of wild-type aggregates. Tips formed within the next

few hours such that the aggregates transformed into finger-shaped structures. The wild-type went on to form fruiting bodies during the next 10 h, but the mutants showed little further morphogenesis during this time (Figure 1). Gradually, over the next day, an increasing number of the mutants culminated and formed short stubby fruiting bodies (Figure 1). However, even after 48 h of development, the efficiency of sporulation was less than 50% of that in wild-type strains.

When induced to develop in unilateral light on low salt agar, conditions that favor slug migration in wild-type strains, cells of strain DG1020 formed fingers that remained in the streak where they had been deposited (Figure 2). The wild-type slugs migrated for long distances leaving few cells in the original streak, but the mutant slugs failed to migrate at all. Because this was the most dramatic gross phenotype of strain DG1020, we named the affected gene *migA*.

Molecular Cloning of migA, a Novel BTB-Domain Gene

Restriction sites in the genomic regions surrounding the plasmid insertion in strain DG1020 were mapped by using a probe from the transformation vector (Figure 3A). Plasmid clones carrying flanking regions were selected in *Escherichia coli* after *Nde*I or *Hin*dIII digestion of genomic DNA prepared from the mutant strain. The sequences of the inserts in these plasmids revealed a large open reading frame (dashed box in Figure 3A). Comparison of the sequence with that of cognate *migA* cDNAs revealed an intron of 98 nucleotides near the 3′ end of the gene and established the polyadenylation site. About 1 kb upstream of *migA*, we encountered the 3′ end of a separate gene that encodes a protein with sequence homology to the peroxisomal acyl-coA oxidase family (GenBank accession no. U87813; stippled box in Figure 3A). All of the regulatory sequences responsible of the expression of *migA* are likely to be located in the 1-kb region between the coding sequences of these genes.

Wild-type cells of strain AX4 were transformed with the *Nde*I plasmid to disrupt *migA* in a fresh strain. Transformants generated by homologous recombination showed the same phenotype observed in the original mutant strain DG1020, confirming that the disruption of the *migA* locus is responsible for the defects in aggregation and migration. One of these recapitulated strains was used in all subsequent experiments.

The open reading frame of *migA* with its 1-kb 5′ untranslated sequence was cloned in a plasmid carrying a gene that confers G418 resistance and transformed into *migA*$^-$ cells. Transformants carrying this construct were found to have a wild-type phenotype, indicating that the cloned region contains the complete *migA* gene and all necessary regulatory components.

The predicted amino acid sequence of MigA is shown in Figure 3B. A 113-aa domain near the N terminus of the protein shows significant homology with portions found at the N terminus of numerous proteins including zinc fingers, poxvirus, and actin binding proteins referred to as the BTB domain, named for the *Drosophila* genes *broad complex*, *tramtrack*, and *bric à brac*, and also known as the POZ domain named for poxviruses and zinc fingers (Bardwell and Treisman, 1994; Zollman *et al.*, 1994; Albagli *et al.*, 1995). This conserved motif appears to function in protein–protein interactions (Bardwell and Treisman, 1994; Chen *et al.*, 1995). Alignment of the N terminus of MigA with several BTB domains shows that the six invariant amino acids defined by Bardwell and Treisman (1994) are conserved in MigA (Figure 4, asterisks). Twenty-nine of the remaining 31 conserved positions recognized by Bardwell and Treisman (1994) are found in the sequence of MigA. The predicted secondary structure of the N-terminal portion of MigA showed alternation of helical and β-sheet structures that were also found in many other BTB domain sequences (Bardwell and Treisman, 1994).

Some of the BTB proteins have been shown to bind actin microfilaments and others have zinc-finger domains implicated in DNA binding (Zollman *et al.*, 1994; Albagli *et al.*, 1995). MigA does not contain any recognizable zinc finger motifs, actin binding motifs, or any other structural or functional motif but has a region near its C terminus with significant similarity to a putative

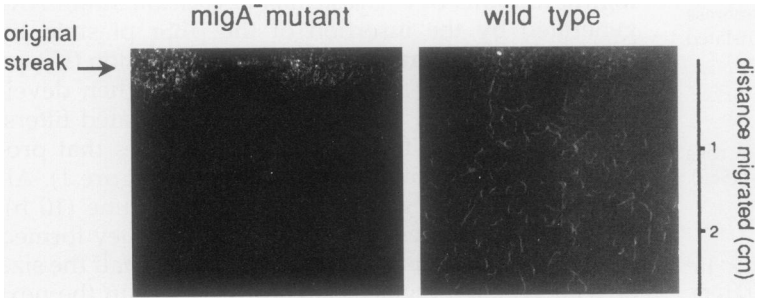

Figure 2. Slug migration. Cells of the *migA*$^-$ mutant strain DG1020 and wild-type strain AX4 were streaked on non-nutrient agar and incubated with unidirectional light for 48 h before being photographed. The position of the original streak and the distance migrated (centimeters) are indicated. The mutant cells failed to form migrating slugs.

protein of unknown function (yk34b1.5) predicted from the genomic sequence of *Caenorhabditis elegans*.

migA$^-$ Cells Are Defective in Chemotaxis

Because *migA*$^-$ mutant cells form small aggregates and slugs that are unable to migrate, we compared the motility and chemotactic properties of single mutant cells at the onset of aggregation to those of wild-type cells at the same stage of development (7 h). Computer-assisted analysis of time-lapse video recordings of cells moving in the absence of any chemotactic gradient showed that the mutant cells were indistinguishable from wild-type cells with respect to size, shape, roundness, or instantaneous velocity of translocation (Table 1). Moreover, the mutant cells changed directions just as frequently as wild-type cells and showed average positive and negative flow statistically indistinguishable from that of wild-type cells. However, analysis of cellular behavior in spatial gradients of the chemoattractant cAMP, generated in a spatial gradient chamber (Zigmond, 1977; Varnum-Finney *et al.*, 1987) revealed that wild-type cells were far more efficient at moving toward the cAMP source than mutant cells (Figure 5). Eighty-five percent of the wild-type cells showed a chemotactic index of +0.2 or better, but only 43% of the *migA*$^-$ cells oriented this well. Moreover, a third of the mutant cells actually moved in a direction away from the source of cAMP (chemotactic indices < 0). The average (±SD) chemotactic index of the parental AX4 cells was $+0.36 \pm 0.39$ (N = 30 cells) and that of the *migA*$^-$ cells was $+0.13 \pm 0.38$ (N = 44 cells). Thus, although the mutant cells are absolutely normal in appearance and can translocate as well as wild-type cells, they are significantly impaired in their ability to direct their movement in response to a spatial gradient of cAMP.

Pulsatile Aggregation

Wild-type cells move toward aggregation centers in a series of surges as they respond to pulsatile waves of chemoattractant initiated at the center and relayed through the population (Alcantara and Monk, 1974; Parent and Devreotes, 1996). We quantitated this behavior over an 8-h period by analyzing video recordings with the newly developed vector flow analysis software described in MATERIALS AND METHODS. Clear peaks began to appear at 5 h of development and increased in amplitude until 8 h of development (Figure 6A). Twenty-six peaks were distinguishable between 5.5 and 8 h, with an average periodicity of 6 min. On the other hand, no indication of velocity peaks were observed during aggregation of *migA*$^-$ cells during this period (Figure 6B). Wild-type cells began to form loose streams at 5.5 h that coalesced into thick stream by 7 h (Figure 6A). In contrast, *migA*$^-$ mutant cells formed aggregates mostly as the result of random cell collisions followed by adhesion of the cells (Figure 6B).

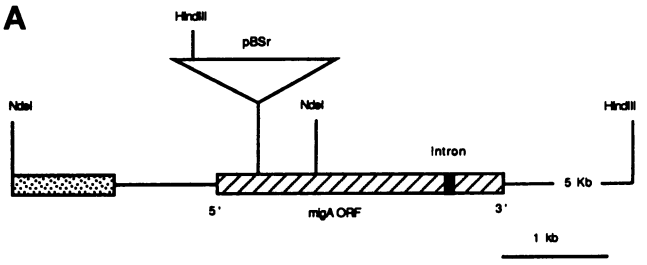

B

```
MATINIINNNNNQNNNNQNNNNNINHTEYFNNGFKSLLGEFKKYTDIKIK  50
CGGQIFPTHRIILANSSEFFGRLLLSDFKESSQSVIELKQPDPFNVFPMV 100
LEFMYDGIIYLSPENVIPLLAMSDHYLIRDLQHLCLLFLDQNLHRENVLT 150
ILKYSIDFHFEPITERCITIISKNFTFVCENLYKQTKINQNNNNNCINIE 200
NNKKHLNTSSASSSLNSSTSSASSSSSSSNNNYYTTTTTTTTTTTASSSN 250
FNKNLTNCKVTGQQQQQQQQQQQQQQQQQQQQQQQQQPIYDFSFLPASIFY 300
QILDHDYLVVNSEYTLYRIVLNFIEKFFGENFTEITYNTNITDQLKVSDL 350
MSQIRYILMPYDQLTLITKDPLIPKEILFETLLERLKRFEGKTSSPSSSS 400
TSSSPSNTSNSPTKQTSPSKYQQQQQQQQQQQQQQQQQQQQQQQQQQQQQ 450
PQQQPQQQPQQPQPQIIQQQPQQPQIIQQQPQQLQQLQQPQQPQTIQQMV 500
QQQQNIQQQQQQQQQQQNIQQQQTQNMQQQLQQQLLQQIQQQQQQQQQPQ 550
IIKQFTPSSSPLSSSFISLNASQSKLSINNATNTTNNNNNNSNNVTNTNN 600
NNIINNNNNNNNNKQTQSNNNDNKILKRYQPRPPQSILFEYSFDFDFKGII 650
FWISTDGGNEKWSNPHSTSKIKITSSSIDKGNLYDIVELTPNAFWTKDVP 700
ASWVMIDLGPNRTVVPMYYTIRHGLSYKSDSLRTWDFQGSTNGEQWTVLK 750
RHTNDPSLNYKYATHSWPVTGCETAFRYFRILQTGKNSNNRNFLVIGGLE 800
IYGELCETNPNPN                                       813
```

Figure 3. *migA* gene and its product. (A) The position of the plasmid insertion and the restriction sites used for cloning are shown over the *migA* open reading frame (ORF; dashed box), which is interrupted by an intron (solid box). The 3′ end of the adjacent gene is located upstream of *migA* (stippled box). (B) The amino acid sequence of the *migA* product was deduced from the nucleotide acid sequence of cDNA and genomic clones (GenBank accession no. U86962). The underlined region at the N terminus is the BTB domain. The underlined region at the C terminus has significant similarity to the uncharacterized product of an ORF found in the *C. elegans* genome (GenBank accession no. U58755).

Behavioral Response to the Rapid Addition of Chemoattractant

The rapid addition of high levels of cAMP (10^{-6} M) to aggregation stage cells causes an immediate inhibition

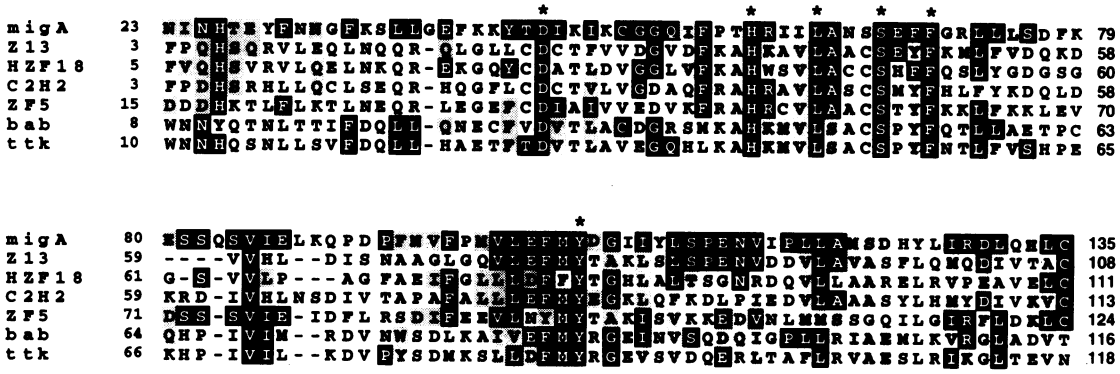

Figure 4. Comparition of BTB domains. The N-terminal domain of MigA was aligned with several mammalian zinc-finger proteins and *Drosophila* proteins by using the Clustal W program. Identical amino acids found in MigA and one of the corresponding sequences are indicated by black-background boxes. Asterisks mark the invariant amino acids of the BTB family. Conserved amino acids are indicated by shaded boxes. Z13, mouse zinc finger (U14556); HZF18, human zinc finger (L16896); C2H2, human zinc finger (U38896); ZF5, mouse zinc finger (L15325); bab, *Drosophila bric a brac* (U01333); ttK, *Drosophila tram-track* (X17121).

of cellular translocation, a transient doubling of F-actin within 10 s, followed by a second slower increase, phosphorylation of myosin, and a redistribution of bundled myosin (Berlot *et al.*, 1985, 1987; Yumura and Fukui, 1985; Nachmias *et al.*, 1989; Wessels *et al.*, 1989; Cox *et al.*, 1992). This procedure has been widely used to determine whether the circuitry between the cAMP receptor and the cytoskeleton is intact (Wessels *et al.*, 1989; Cox *et al.*, 1992). The average instantaneous velocity of 50 wild-type cells and 80 mutant cells was measured during a 5-min period before the addition of 10^{-6} M cAMP, for 1 min while cAMP was present, and for at least 15 min after the removal of cAMP. The average instantaneous velocity of both wild-type and mutant cells decreased by 50% immediately after the addition of cAMP and rebounded quickly after its removal (Figure 7). If cAMP was not removed, both wild-type and mutant cells partially rebounded in identical manners (our unpublished results). When 10^{-7} M cAMP was added and not removed, instantaneous velocity decreased and then returned to normal in both wild-type and mutant cells with the same kinetics previously described by Varnum-Finney *et al.* (1987) (our unpublished results). These results suggest that the circuitry between the cAMP receptor and the cytoskeleton functions normally when *migA*$^-$ cells are treated with a concentration of cAMP that rapidly saturates surface receptors (Klein and Juliani, 1977; Wang *et al.*, 1988). To further characterize this response, the level of F-actin was determined before and after the addition of 10^{-6} M cAMP. The amount of F-actin doubled within 10 s, decreased to the resting-state level, and then increased again between 20 and 90 s in both wild-type and mutant cells (our unpublished results). Nevertheless, *migA*$^-$ cells are not able to accurately assess the direction of chemoattractant in a relatively stable spatial gradient of cAMP or in a natural aggregation territory where gradually increasing and decreasing concentrations of cAMP pass over them.

Expression of Cell Type-specific Markers in migA$^-$ Cells

To further define the developmental phenotype of *migA*$^-$ mutant cells, the pattern and the level of expression of different cell type-specific markers were

Table 1. Motility parameters of a parental Ax4 and migA$^-$ cells perfused with buffer or responding to a gradient of chemoattractant

Condition	Strain	No. cells	Inst. vel. (μm/min)	Dir. ch. (deg)	Pos. flow (% per)	Neg. flow (% per)	Max. length (μm)	Max. width (μm)	Mean width (μm)	Roundness (%)
Buffer	Ax4	31	9.8 ± 3.2	40.5 ± 9.3	14.2 ± 7.1	13.2 ± 7.4	17.6 ± 3.7	5.7 ± 1.10	4.5 ± 0.9	50.4 ± 10.5
	migA$^-$	40	10.1 ± 4.4	38.4 ± 10.8	15.2 ± 7.2	15.8 ± 7.7	17.4 ± 4.1	5.6 ± 1.1	4.1 ± 1.0	45.2 ± 12.6
(p value)			(NS)		(NS)	(NS)	(NS)	(NS)	(NS)	(NS)
cAMP gradient	Ax4	30	10.1 ± 1.0	31.8 ± 9.0	13.6 ± 2.2	13.7 ± 2.1	18.9 ± 2.7	6.4 ± 0.8	4.4 ± 0.6	47.3 ± 8.2
	migA$^-$	44	10.0 ± 2.3	34.7 ± 11.3	11.2 ± 3.2	11.6 ± 2.9	17.7 ± 2.1	5.4 ± 0.6	4.2 ± 1.0	46.0 ± 8.1
(p value)			(NS)		(0.042)	(NS)	(NS)	(NS)	(NS)	(NS)

Inst. vel., instantaneous velocity; Dir. ch., directional change; Pos. flow, positive flow; Neg. flow, negative flow; Max length, maximum length; Max. width, maximum width; NS, not significant. See Soll (1995) for formulas of these parameters. Data are the means ± SE.

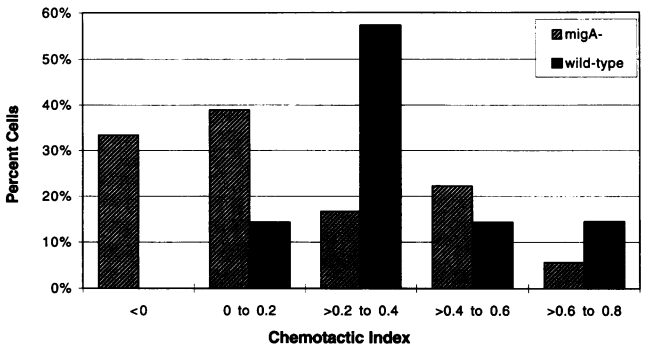

Figure 5. Chemotaxis to cAMP. Wild-type cells of strain AX4 (solid bars) and *migA*$^-$ cells (hatched bars) were distributed on the bridge of the spatial gradient chamber that is bordered by parallel troughs. One trough was filled with BSS alone (sink) and the other was filled with BSS containing 1 μM cAMP (source). After 8 min, cellular behavior was video recorded for 10 min, and the chemotactic index (CI) was calculated as described in MATERIALS AND METHODS. A high proportion of *migA*$^-$ cells exhibited a chemotactic index (CI) that was negative or close to 0.

determined. Accumulation of mRNA from the prestalk genes *ecmA* and *ecmB* and the prespore gene *cotB* was visualized at the finger and culmination stages by in situ hybridization with appropriate probes (Figure 8). At the finger stage, *ecmA* was found in cells at the anterior and in cells scattered throughout the prespore region, whereas *ecmB* was present in a small group of cells in the core of the prestalk region and in the anterior-like cells scattered throughout the back. Prespore cells that stained for *cotB* mRNA were localized to the posterior two-thirds. These patterns of cell type-specific markers do not differ from those obtained at this stage in wild-type strains (Escalante and Loomis, 1995). However, the patterns seen in mutant culminants had several abnormalities (Figure 8). Both *ecmA* and *ecmB* mRNA were found in cells near the top of the stalk tube and in the basal disk but were absent in cells toward the base of the stalk. The most striking difference from wild-type culminants was the absence of *ecmB* staining in the cells surrounding the sorus. In wild-type strains, cells of the upper and lower cups express *ecmB* (Escalante and Loomis, 1995). Either these cell types are missing or they are not expressing the normal complement of genes. These alterations in the prestalk-specific pattern of expression may be related to the delay in culmination and subsequent abnormalities seen in *migA*$^-$ strains.

Northern blot analyses of the accumulation of mRNA from these genes confirmed that they are all expressed at the same level as found in wild-type cells at 12 h of development but fail to accumulate to wild-type levels by 16 h of development (Figure 9). Reduced levels of accumulation in the mutant cells was also seen for another prespore specific gene, *wacA*, that encodes a protein similar to aquaporins (Flick *et al.*, 1997; Figure 9). To determine whether *migA*$^-$ cells were responsive to cAMP, they were shaken in buffer for 6 h, and then 300 μM cAMP was added to half while the remainder were kept in buffer. Those incubated with cAMP received further additions of cAMP to 150 μM every 2 h. Six hours after the addition of cAMP, all the cells were collected and total RNA was prepared. Northern blot analyses showed that cells incubated in the absence of cAMP failed to express either *ecmA* or *cotB* and those incubated in the presence of cAMP accumulated these mRNAs to levels comparable to those found in wild-type cells treated in a similar manner. These results indicate that postaggregative *migA*$^-$ cells respond normally to cAMP by expressing cell type-specific genes.

The Consequences of Disruption of migA Are Cell Autonomous

To allow us to recognize *migA*$^-$ cells in mixtures with wild-type cells, the *migA* gene was knocked out in a strain carrying the *lacZ* gene reporter under the control of actin 15 promoter that is expressed in all cells during growth such that β-galactosidase accumulates and can be recognized by staining with X-gal. We mixed such cells with an equal number of cells of strain AX4 and allowed then to coaggregate. When streams were first formed, the stained cells were seen only at the edges as if they were late in arriving or were being excluded (Figure 10A). At later stages, some mutant cells could be seen to have entered into mixed aggregates but they remained at the back (Figure 10, B and C). If such chimeric slugs migrated, most of the mutant cells were left behind. However, a few stained cells could be seen incorporated at the back of migrating slugs (Figure 10D). When these structures culminated, the mutant cells were found at the bottom of the sorus (Figure 10E). In contrast, *migA*$^+$ cells of the host strain that carries act15::lacZ were found throughout slugs and fruiting bodies when mixed with equal numbers of AX4 cells (Figure 10F).

These experiments were confirmed by using *migA*$^-$ cells carrying the prespore specific marker cotB::lacZ (our unpublished results). When these cells were mixed with wild-type cells, most of the stained cells were found to have been left behind when slugs crawled away. A few stained cells were seen in migrating slugs but these were all at the back. These results suggest that mutation of the *migA* gene results in a cell autonomous defect in the cells so that they do not aggregate as well as the wild-type and are relegated to the edges of streams. From there they can only take up positions at the back of the slug.

migA Is a Developmentally Regulated Gene

Poly(A)$^+$ RNA was prepared from wild-type and mutant cells at different stages of development and elec-

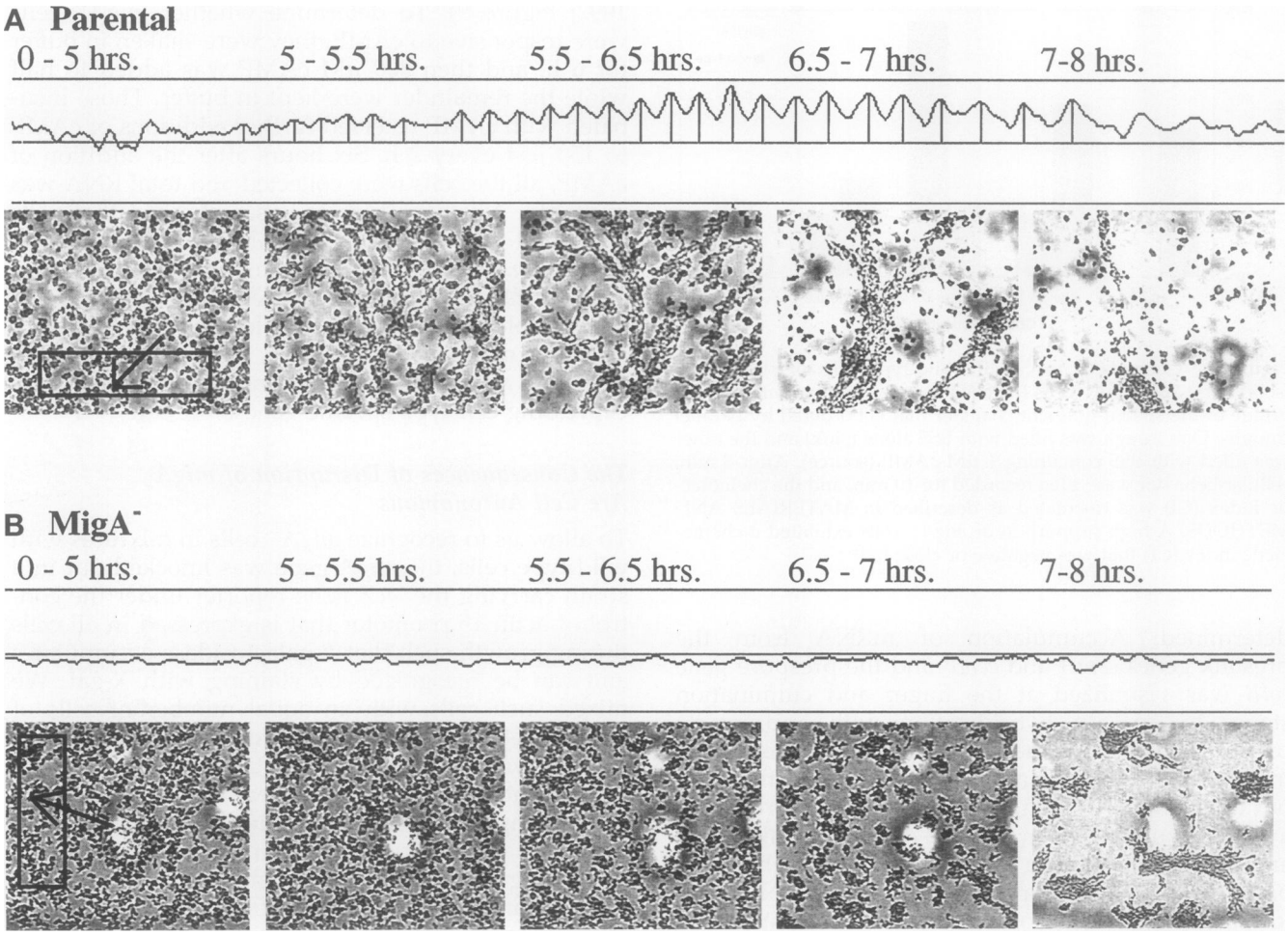

Figure 6. Pulsatile chemotaxis in natural aggregation territories. Video recordings of aggregating wild-type or mutant cells were frame-grabbed into a Macintosh Power PC at 20-s intervals and subject to vector flow analysis as described in MATERIALS AND METHODS. A series of images at selected time points between 0 and 8 h of aggregation are presented for parental cells (A) and *migA*$^-$ cells (B). Results of the vector flow analysis are presented as a time line above the corresponding images. Clear surges and peaks in directional velocity are apparent in the vector flow graph of wild-type cells but are notably absent in mutants. The results presented are representative of five independent experiments. In the vector analysis of aggregating *migA*$^-$ cells, the arrow was rotated through 360°, but pulses were never detected. The time-lapse analyses demonstrated that *migA*$^-$ cells do not form aggregates as a result of surges in directional velocity.

trophoretically separated on agarose gels. Northern blots of these gels were probed for *migA* mRNA (Figure 11). A 2.9-kb mRNA was first detected at low levels after 4 h of development in wild-type cells. It increased to a maximum at 8 h and then remained high throughout the remainder of development (Figure 11). At early stages, a slightly higher band could be seen that disappeared by 8 h of development. Neither of these bands were seen in RNA prepared from *migA*$^-$ cells, suggesting that they are null mutants. To confirm that the phenotype results from the complete lack of MigA protein, we generated a strain in which the *migA* gene was deleted (see MATERIALS AND METHODS). This strain has exactly the same phenotype as those in which the *migA* gene is disrupted by plasmid insertion.

Cell-Type Specificity of Expression of migA

Although *migA* mRNA could be recognized as a weak band on Northern blots of total RNA, the level was too low for definitive localization by in situ hybridization. Therefore, we prepared a construct in which LacZ was fused in-frame to MigA after the first 130 codons. This construct carries the complete *migA* upstream region as well as the 3′ end of the adjacent gene (see Figure 3A). Wild-type cells transformed with this construct were stained at various times during development (Figure 12A). All of the cells in loose mounds were stained, indicating a lack of cell-type specificity at this stage. However, at the tipped mound stage (12 h of development), most of the stained cells were seen in the tip. Thereafter, only prestalk cells were stained

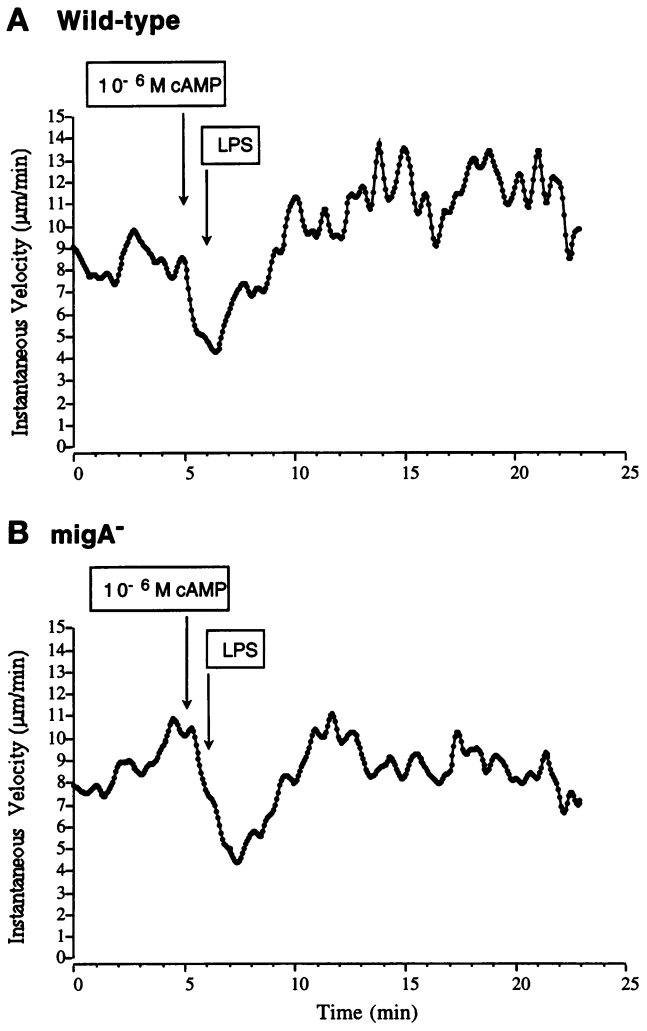

Figure 7. Motility response to high levels of cAMP. Instantaneous velocity plots of AX4 wild-type cells (A) and *migA*$^-$ cells (B) demonstrate that *migA*$^-$ cells respond normally to the rapid addition of a high concentration of cAMP. Cells of mutant and wild-type strains were plated at low density in a Sykes-Moore chamber and video recorded for 5 min while being perfused with BSS alone. The perfusion solution was then switched to BSS containing 1 μM cAMP for 1 min. The cells were subsequently perfused with BSS alone. The average instantaneous velocity for 50 AX4 and 80 *migA*$^-$ cells in three or four independent experiments, respectively, was calculated and plotted by using 2D-DIAS. The plots were smoothed five times by using a suitable Tukey Window. The time of shift from buffer to cAMP and back to BSS is indicated by the arrows.

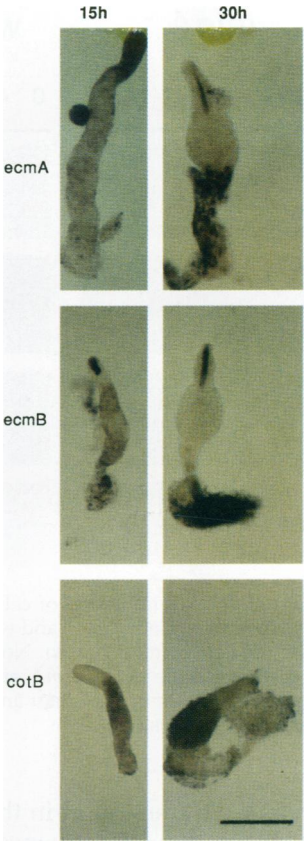

Figure 8. In situ localization of cell type-specific markers. Cells of a *migA*$^-$ strain were fixed and hybridized with riboprobes from the prestalk genes *ecmA* and *ecmB* and the prespore gene *cotB* after 15 h and 30 h of development. Bar, 0.2 mm.

indicating that the β-galactosidase fusion protein that had been expressed earlier was unstable in prespore cells. This finding was somewhat surprising because β-galactosidase is normally very stable after being synthesized in *Dictyostelium* (Detterbeck *et al.*, 1994). However, we were looking at a fusion protein in which the first 130 aa were encoded by the BTB domain of *migA* which might affect the stability of the entire protein. Therefore, we prepared another construct in which *lacZ* was fused after the second codon of *migA*. Wild-type cells transformed with this construct were stained at various times in development (Figure 12B). Unlike the transformants with the previous construct, both prespore and prestalk cells in culminants were stained. However, the staining was more intense in prestalk cells. It appears that when the N terminus of MigA that includes the BTB domain is present, the protein is unstable in prespore cells such that by the time fingers are formed it is only found in prestalk cells. It is possible that MigA is also unstable in prestalk cells but is continually replenished as the result of prestalk-specific expression of *migA*.

DISCUSSION

The *migA* gene of *Dictyostelium* is first expressed as cells develop the ability to chemotactically respond to gradients of cAMP. Its 2.9-kb mRNA accumulates between 4 and 8 h after the initiation of development and persists until fruiting-body formation. The predicted product is a protein of 94 kDa with a BTB domain near the N terminus that may function in protein–protein interactions. At the C terminus, there is a sequence that is highly related to one predicted to be encoded by an otherwise uncharacterized open

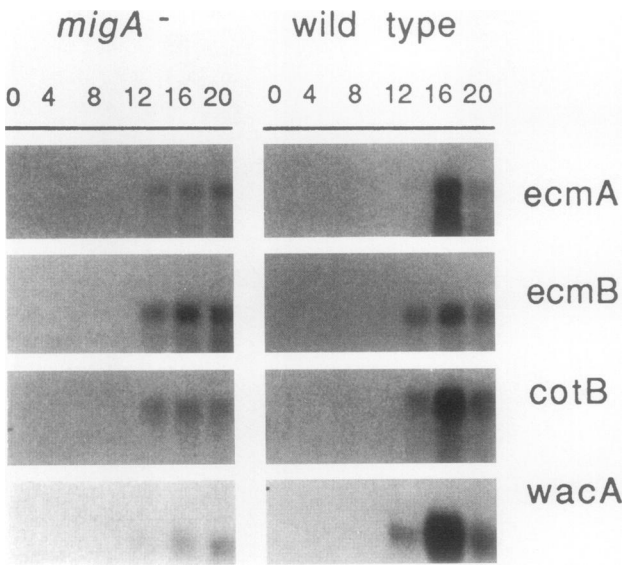

Figure 9. Accumulation of cell type-specific mRNAs. Total RNA was prepared from *migA*$^-$ and wild-type cells after development for the indicated times (hours). Northern blots were probed with the prestalk-specific genes *ecmA* and *ecmB* and the prespore-specific genes *cotB* and *wacA*. Mutant and wild-type blots were probed and exposed identically.

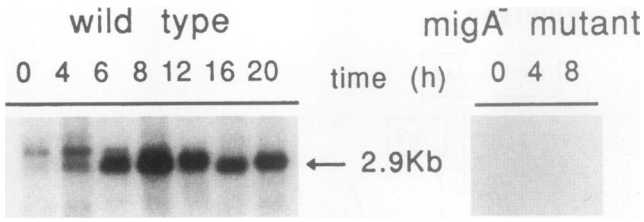

Figure 11. Accumulation of *migA* mRNA during development. Poly(A)$^+$ RNA was prepared at the indicated times in development (hours) from wild-type and *migA*$^-$ cells. Northern blots were hybridized with a *migA* probe.

reading frame found in the genome of *C. elegans*. This conservation of sequence suggests that these genes play an evolutionarily conserved role.

When the initial cell types differentiate after aggregation, MigA appears to be retained only in prestalk cells. A fusion protein in which the N-terminal portion of MigA is fused to β-galactosidase of *E. coli* accumulates in all cells of loose aggregates but then is degraded in prespore cells while remaining in prestalk cells. Deleting all but two of the MigA-encoded amino acids from this construct results in the accumulation of β-galactosidase in both cell types. These results indicate that the N-terminal domain of MigA is responsible for restricting accumulation to prestalk cells as they sort out to the anterior. Slug migration is directed by cells at the anterior and can be blocked by preferentially inhibiting protein synthesis in prestalk cells (Francis, 1964; Shaulsky and Loomis, 1993). Therefore, it is not surprising that MigA plays a role in slug migration.

We initially picked DG1020, the strain in which *migA* was tagged, because the slugs looked aberrant. Tips formed at the anterior but the slugs failed to migrate and stalk formation was both delayed and reduced. Further analysis showed that aggregation was also aberrant in *migA*$^-$ mutant strains. By using two-dimensional computer-assisted motion analysis, we were able to show that the chemotactic index of *migA*$^-$ mutant cells to gradients of cAMP was only about a third of that in wild-type cells. Similar reduc-

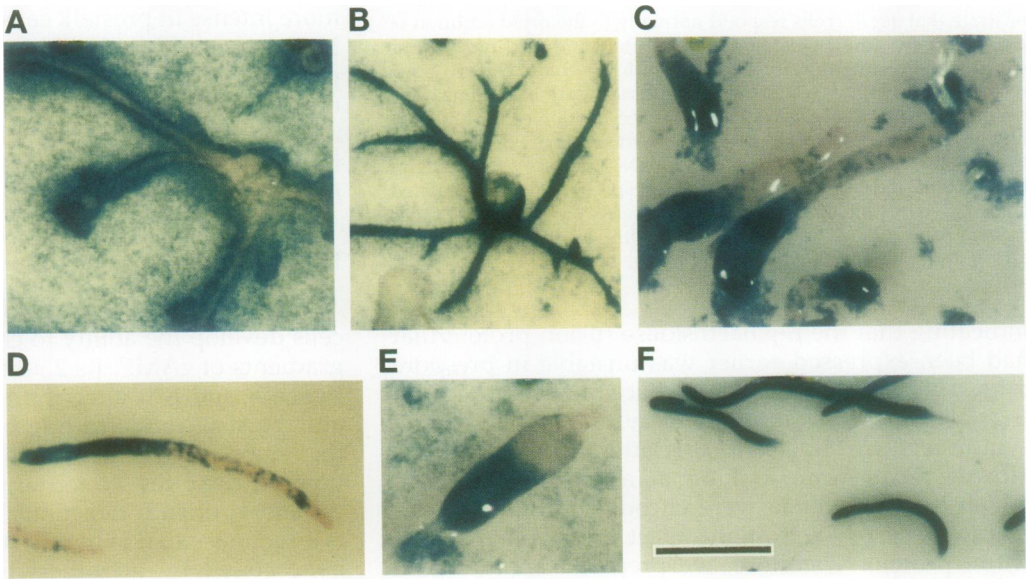

Figure 10. Localization of *migA*$^-$ cells in chimeric structures. *migA*$^-$ mutant cells carrying *act15::lacZ* were mixed with an equal number of wild-type cells and developed on filters for 10 h (A), 12 h (B), 14 h (C), and 20 h (E). The mutant cells were stained blue with X-gal. Mixtures of these strains were also developed on agar with unidirectional light and migrating slugs were stained after 48 h (D). Migrating slugs formed from a mixture of *migA*$^+$ *act15::lacZ* and wild-type cells are shown for comparison (F). Bar, 0.2 mm.

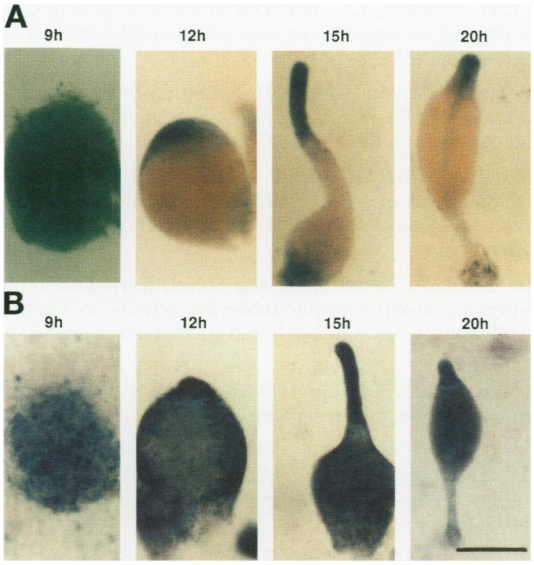

Figure 12. Localization of *migA* expression. (A) Cells of a strain transformed with a construct in which the upstream region and 130 codons of the *migA* ORF was fused to *lacZ* were developed for the indicated times (hours) and stained with X-gal. (B) Cells of a strain transformed with a construct in which the upstream region had only three codons of the *migA* ORF fused to *lacZ* were developed for the indicated times (hours) and stained with X-gal. Bar, 0.2 mm.

tions in chemotactic indices have been observed in cytoskeletal mutants lacking either myosin II heavy chain or the actin cross-linking protein gp120 (Wessels *et al.*, 1988; Cox *et al.*, 1992, 1996). However, translocation is also dramatically reduced in cells of these strains, whereas it is completely normal in *migA*$^-$ cells. *migA*$^-$ cells have the same instantaneous velocity and persistence of translocation as wild-type cells. Moreover, they are the same size and shape. Their basic capacity to crawl appears intact but they are seriously impaired in their ability to read a gradient. This defect could be seen in the absence of surges in natural aggregation territories. Cyclic behavior began in wild-type populations at 5 h of development as the cells responded to outwardly moving nondissipating waves of cAMP (Alcantara and Monk 1974; Parent and Devreotes, 1996). The period between cyclic increases in velocity toward aggregation centers averaged 6 min and maximum amplitude was achieved at 7 h as wild-type cells entered streams. In contrast, *migA*$^-$ cells never showed cyclical surges in any direction although they were able to form small aggregates by random collision followed by adhesion. This aberrant behavior might be the consequence of an inability of *migA*$^-$ cells to read gradients of cAMP and/or to their inability to relay the cAMP signal. Although the ability of *migA*$^-$ mutant cells to assess a spatial gradient or to move in surges to aggregation centers in natural territories is clearly impaired, they respond to the rapid addition of either 10^{-7} M or 10^{-6} M cAMP, the peak concentration in natural waves, in a normal manner. Actin polymerization in response to 10^{-6} M cAMP is also normal in the mutant cells. The rapid reduction in velocity and the increase in actin polymerization in response to high levels of cAMP have been taken as evidence that the circuitry between the cAMP receptor and the cytoskeleton is intact. However, cAMP increases and decreases in a more gradual manner in natural waves and it is possible that *migA*$^-$ cells respond differently under those conditions.

When *migA*$^-$ cells were allowed to develop in the presence of wild-type cells, they coaggregated but most of the mutant cells were relegated to the edges of the streams, indicating that the consequences of loss of MigA are cell autonomous during aggregation. When a few mutant cells were incorporated into predominantly wild-type slugs, they were seen to be at the back and to be left behind when the slugs migrated. Thus, the defects in migration are also cell autonomous.

In situ hybridization of cell type-specific gene products showed that prestalk cells sorted out normally in pure populations of *migA*$^-$ cells so that they were predominantly found at the anterior during the finger stage. However, the prestalk marker *ecmB* was not expressed in the upper or lower cups that cradle the sorus during culmination. Thus, prestalk cell gene expression appears to be affected during terminal differentiation of *migA*$^-$ mutant cells. Moreover, Northern blot analyses showed that the level of accumulation of both prespore- and prestalk-specific genes during culmination is reduced, perhaps as a consequence of the overall defects in morphogenesis.

There are at least four stages during morphogenesis of *Dictyostelium* in which the direction of cell movement is critical: aggregation when cells must move to collecting centers; sorting out when prestalk cells must move to the tip; slug migration when cells at the tip must move forward; and culmination when prestalk cells have to move down through underlying prespore cells. Mutants in which the *migA* gene is disrupted or deleted appear to be impaired in two of these processes. Cells of these strains have significantly reduced abilities to respond to a chemotactic gradient of cAMP and cannot migrate as slugs. However, they can differentiate into prestalk cells that sort out to the tip and subsequently form stalks, albeit short and misformed ones.

The processes of relative cell movement at the different stages appear to be quite different and might be completely independent. During aggregation cells move on a substratum and respond to chemotactic gradient of cAMP as separate individuals. Sorting out of prestalk cells may involve responses to cAMP but appears to be unimpaired in *migA*$^-$ mutants. During

slug migration, prestalk cells at the anterior move in a spiral manner and distend the extracellular matrix (Francis, 1964; Siegert and Weijer, 1995). When fruiting body formation is initiated, prestalk cells vacuolize and expand within a stalk tube that is pushed down until it hits the substratum. This process appears to be unimpaired in *migA*$^-$ mutants. Cells lacking MigA can translocate perfectly well and can sense and respond to cAMP in a variety of ways that are coupled to receptor occupancy. Thus, it is unlikely that the signal transduction pathway that signals the relative concentration of cAMP around a cell is affected by the mutation. More likely, MigA plays an essential role at a later step in which the direction of cell movement is determined. Pulses of cAMP clearly provide the directional signals in a chemotactic field and may do so as well as in the tip of a slug. However, there is evidence that extracellular cAMP is not essential for differentiation or slug migration (Abe and Yanagisawa, 1983; Wang and Kuspa, 1997). It is possible that a distinct mechanism generates the signals that control postaggregative cellular movement that are ignored by *migA*$^-$ mutants.

ACKNOWLEDGMENTS

We thank Dr. Nir Osherov for the isolation of strain DG1020 and Negin Iranfar and Dianne Foster for sequencing. We also thank Nick Von Bergen for technical assistance. R.E. was the recipient of a MEC/Fulbright Scholarship. This work was supported by the Developmental Gene Program (NICHD-30892) to W.F.L. and grant HD-18577 to D.R.S.

REFERENCES

Abe, K., and Yanagisawa, K. (1983). A new class of rapid developing mutants in *Dictyostelium discoideum*: implications for cyclic AMP metabolism and cell differentiation. Dev. Biol. *95*, 200–210.

Adachi, H., Hasebe, T., Yoshinaga, K., Ohta T., and Sutoh, K. (1994). Isolation of *Dictyostelium discoideum* cytokinesis mutants by restriction enzyme-mediated integration of the blasticidin S resistance marker. Biochem. Biophys. Res. Commun. *205*, 1808–1814.

Albagli, O., Dhordain, P., Deweindt, C., Lecocq, G., and Leprince, D. (1995). The BTB/POZ domain: a new protein-protein interaction motif common to DNA-and Actin-binding proteins. Cell Growth & Differ. *6*, 1193–1198.

Alcantara, F., and Monk, M. (1974). Signal propagation during aggregation in the slime mould *Dictyostelium discoideum*. J. Gen. Microbiol. *85*, 321–334.

Altschul, S., Miller, W., Myers, E., and Lipman, D. (1990). Basic local alignment search tool. J. Mol. Biol. *215*, 403–410.

Ausubel, F.M., Brent, R., Kingston, R.E., Moore, D.D., Seidman, J.G., Smith, J.A., and Struhl, K. (1992). Current Protocols in Molecular Biology, New York: John Wiley & Sons.

Bardwell, V.J., and Treisman, R. (1994). The POZ domain: a conserved protein-protein interaction motif. Genes Dev. *8*, 1664–1677.

Berlot, C.H., Devreotes, P.N., and Spudich, J.A. (1987). Chemoattractant elicited increases in *Dictyostelium* myosin phosphorylation are due to changes in myosin localization and increases in kinase activity. J. Biol. Chem. *262*, 3918–3926.

Berlot, C.H., Spudich, J.A., and Devreotes, P.N. (1985). Chemoattractant-elicited increases in myosin phosphorylation in *Dictyostelium*. Cell *43*, 307–314.

Bonner, J., and Williams, J. (1994). Inhibition of cAMP-dependent protein kinase in *Dictyostelium* prestalk cells impairs slug migration and phototaxis. Dev. Biol. *164*, 325–327.

Bretschneider, T., Siegert, F., and Weijer, C.J. (1995). Three-dimensional scroll waves of cAMP could direct cell movement and gene expression in *Dictyostelium* slugs. Proc. Natl. Acad. Sci. USA *92*, 4387–4391.

Chandrasekhar, A., Wessels, D., and Soll, D.R. (1995). A mutation that depresses cGMP phosphodiesterase activity in *Dictyostelium* affects cell motility through an altered chemotactic signal. Dev. Biol. *169*, 109–122.

Chen, M.Y., Insall, R.H., and Devreotes, P.N. (1996). Signaling through chemoattractant receptors in *Dictyostelium*. Trends Genet. *12*, 52–57.

Chen, W., Zollman, S., Couderc, J.L., and Laski, F.A. (1995). The BTB domain of bric a brac mediates dimerization in vitro. Mol. Cell. Biol. *15*, 3424–3429.

Cox, D., Condeelis, J., Wessels, D., Soll, D., Kern, H., and Knecht, D.A. (1992). Targeted disruption of the ABP-120 gene leads to cells with altered motility. J. Cell Biol. *116*, 943–955.

Cox, D., Wessels, D., Soll, D.R., Hartwig, J., and Condeelis, J. (1996). Re-expression of ABP-120 rescues cytoskeletal, motility, and phagocytosis defects of ABP-120(-) *Dictyostelium* mutants. Mol. Biol. Cell *7*, 803–823.

Detterbeck, S., Morandini, P., Wetterauer, B., Bachmair, A., Fischer, K., and MacWilliams, H.K. (1994). The "prespore-like cells" of *Dictyostelium* have ceased to express a prespore gene: Analysis using short-lived beta- galactosidases as reporters. Development *120*, 2847–2855.

Escalante, R., and Loomis, W.F. (1995). Whole-mount in situ hybridization of cell-type-specific mRNAs in *Dictyostelium*. Dev. Biol. *171*, 262–266.

Firtel, R.A. (1995). Integration of signaling information in controlling cell- fate decisions in *Dictyostelium*. Genes Dev. *9*, 1427–1444.

Flick, K.M., Shaulsky, G., and Loomis, W.F. (1997). The *wacA* gene of *Dictyostelium discoideum* is a developmentally regulated member of the MIP family. Gene (*in press*).

Fosnaugh, K.L., and Loomis, W.F. (1989). Spore coat genes SP60 and SP70 of *Dictyostelium discoideum*. Mol. Cell. Biol. *9*, 5215–5218.

Francis, D.W. (1964). Some studies on phototaxis of *Dictyostelium*. J. Cell. Comp. Physiol. *64*, 131–138.

Hall, A.L., Schlein, A., and Condeelis, J. (1988). Relationship of pseudopod extension to chemotactic hormone-induced actin polymerization in amoeboid cells. J. Cell. Biochem. *37*, 285–299.

Harwood, A.J., and Drury, L. (1990). New vectors for expression of the *E. coli lacZ* gene in *Dictyostelium*. Nucleic Acids Res. *18*, 4292.

Harwood, A.J., Hopper, N.A., Simon, M.N., Bouzid, S., Veron, M., and Williams, J.G. (1992). Multiple roles for cAMP-dependent protein kinase during *Dictyostelium* development. Dev. Biol. *149*, 90–99.

Insall, R., Kuspa, A., Lilly, P.J., Shaulsky, G., Levin, L.R., Loomis, W.F., and Devreotes P. (1994). CRAC, a cytosolic protein containing a pleckstrin homology domain, is required for receptor and G protein-mediated activation of adenylyl cyclase in *Dictyostelium*. J. Cell Biol. *126*, 1537–1545.

Jermyn, K.A., Duffy, K.T., and Williams, J.G. (1989). A new anatomy of the prestalk zone in *Dictyostelium*. Nature *340*, 144–146.

Klein, P., and Juliani, M. (1977). cAMP-induced changes in cAMP-binding sites in *D. discoideum* amoebae. Cell *10*, 329–335.

Kuspa, A., and Loomis, W.F. (1992). Tagging developmental genes in *Dictyostelium* by restriction enzyme-mediated integration of plasmid DNA. Proc. Natl. Acad. Sci. USA *89*, 8803–8807.

Kuwayama, H., Ishida, S., and Van Haastert, P.J.M. (1993). Non-chemotactic *Dictyostelium discoideum* mutants with altered cGMP signal transduction. J. Cell Biol. *123*, 1453–1462.

Loomis, W.F. (1975). Polarity and pattern in *Dictyostelium*. In: Developmental Biology: Pattern Formation, Gene Regulation (ICN-UCLA Symposium), ed. D. McMahon and C.F. Fox, Menlo Park, CA: W.A. Benjamin, 109–128.

Loomis, W.F. (1982). The Development of *Dictyostelium discoideum*, New York: Academic Press.

Loomis, W.F. (1996). Genetic networks that regulate development in *Dictyostelium* cells. Microbiol. Rev. *60*, 135–150.

Manstein, D.J., Schuster, H.P., Morandini P., and Hunt, D.M. (1995). Cloning vectors for the production of proteins in *Dictyostelium discoideum*. Gene *162*, 129–134.

Nachmias, V.T., Fukui, Y., and Spudich, J.A. (1989). Chemoattractant-elicited translocation of myosin in motile *Dictyostelium*. Cell Motil. Cytoskeleton *13*, 158–169.

Parent, C.A., and Devreotes, P.N. (1996). Constitutively active adenylyl cyclase mutant requires neither G proteins nor cytosolic regulators. J. Biol. Chem. *271*, 18333–18336.

Reymond, C.D., Schaap, P., Veron, M., and Williams, J.G. (1995). Dual role of cAMP during *Dictyostelium* development. Experientia *51*, 1166–1174.

Sambrook, J., Fritsch, E.F., and Maniatis, T. (1989). Molecular Cloning: A Laboratory Manual, 2nd ed., Plainview, NY: Cold Spring Harbor Laboratory Press.

Schnitzler, G.R., Fischer, W.H., and Firtel, R.A. (1994). Cloning and characterization of the G-box binding factor, an essential component of the developmental switch between early and late development in *Dictyostelium*. Genes Dev. *8*, 502–514.

Shaulsky, G., Kuspa, A., and Loomis, W.F. (1995). A multidrug resistance transporter serine protease gene is required for prestalk specialization in *Dictyostelium*. Genes Dev. *9*, 1111–1122.

Shaulsky, G., and Loomis, W.F. (1993). Cell type regulation in response to expression of ricin-A in *Dictyostelium*. Dev. Biol. *160*, 85–98.

Siegert, F., and Weijer, C.J. (1992). Three-dimensional scroll waves organize *Dictyostelium* slugs. Proc. Natl. Acad. Sci. USA *89*, 6433–6437.

Siegert, F., and Weijer, C.J. (1995). Spiral and concentric waves organize multicellular *Dictyostelium* mounds. Curr. Biol. *5*, 937–943.

Soll, D.R. (1987). Methods for manipulating and investigating developmental timing in *Dictyostelium discoideum*. Methods Cell Biol. *28*, 413–431.

Soll, D.R. (1995). The use of computers in understanding how animal cells crawl. Int. Rev. Cytol. *163*, 43–104.

Soll, D.R., and Voss, E. (1997). Two and three dimensional computer systems for analyzing how animal cells crawl. In: The Motion Analysis of Living Cells, ed. D.R. Soll and D. Wessels, New York: John Wiley & Sons (*in press*).

Sussman, M. (1987). Cultivation and synchronous morphogenesis of *Dictyostelium* under controlled experimental conditions. Methods Cell Biol. *28*, 9–29.

Traynor, D., Kessin, R.H., and Williams, J.G. (1992). Chemotactic sorting to cAMP in the multicellular stages of *Dictyostelium* development. Proc. Natl. Acad. Sci. USA *89*, 8303–8307.

Varnum, B., Edwards, K.B., and Soll, D.R. (1986). The developmental regulation of single-cell motility in *Dictyostelium discoideum*. Dev. Biol. *113*, 218–227.

Varnum, B., and Soll, D.R. (1984). Effects of cAMP on single cell motility in *Dictyostelium*. J. Cell Biol. *99*, 1151–1155.

Varnum-Finney, B., Edwards, K.B., Voss, E., and Soll, D.R. (1987). Amoebae of *Dictyostelium discoideum* respond to an increasing temporal gradient of the chemoattractant cAMP with a reduced frequency of turning: Evidence for a temporal mechanism in amoeboid chemotaxis. Cell Motil. Cytoskeleton *8*, 7–17.

Wang, B., and Kuspa, A. (1997). *Dictyostelium* development in the absence of cAMP. Science *277*, 251–254.

Wang, M., Van Haastert, P.J.M., Devreotes, P.N., and Schaap, P. (1988). Localization of chemoattractant receptors on *Dictyostelium discoideum* cells during aggregation and down-regulation. Dev. Biol. *128*, 72–77.

Wessels, D., Schroeder, N.A.,Voss, E., Hall, A.L., Condeelis, J., and Soll, D.R. (1989). cAMP-mediated inhibition of intracellular particle movement and actin reorganization in *Dictyostelium*. J. Cell Biol. *109*, 2841–2851.

Wessels, D., Soll, Knecht, D.R., D., Loomis, W.F., De Lozanne, A., and Spudich, J. (1988). Cell motility and chemotaxis in *Dictyostelium* amoebae lacking myosin heavy chain. Dev. Biol. *128*, 164–177.

Williams, J.G., Duffy, K.T., Lane, D.P., McRobbie, S.J., Harwood, A.J., Traynor, D., Kay, R.R., and Jermyn, K.A. (1989). Origins of the prestalk-prespore pattern in *Dictyostelium* development. Cell *59*, 1157–1163.

Williams, J.G., and Jermyn, K.A. (1991). Cell sorting and positional differentiation during *Dictyostelium* morphogenesis. In: Cell-Cell Interactions in Early Development, ed. J. Gerhart, New York: Wiley-Liss, 261–272.

Yumura, S., and Fukui, Y. (1985). Reversible cAMP-dependent change in distribution of myosin thick filaments in *Dictyostelium*. Nature *314*, 194–196.

Zigmond, S.H. (1977). The ability of polymorphonuclear leukocytes to orient in gradients of chemotactic factors. J. Cell Biol. *75*, 606–616.

Zollman, S., Godt, D., Prive, G.G., Couderc, J.L., and Laski, F.A. (1994). The BTB domain, found primarily in zinc finger proteins, defines an evolutionarily conserved family that includes several developmentally regulated genes in *Drosophila*. Proc. Natl. Acad. Sci. USA *91*, 10717–10721.